ACADEMIC PRESS

Available online at www.sciencedirect.com

SCIENCE DIRECT®

Journal of Sound and Vibration 262 (2003) 795–813

JOURNAL OF SOUND AND VIBRATION

www.elsevier.com/locate/jsvi

Boundary control of an axially moving string via fuzzy sliding-mode control and fuzzy neural network methods

Paul C.-P. Chao*, Cheng-Liang Lai

Department of Mechanical Engineering, Chung Yuan Christian University, Chung-Li, Taiwan 32023, ROC

Received 4 May 2001; accepted 21 June 2002

Abstract

The objective of this study is to develop intelligent control schemes for the transverse vibration reduction of an axially moving string. The proposed approaches are backboned by the methods of fuzzy sliding-mode control (FSMC) and fuzzy neural network control (FNNC). In practice, the control effort for the system is realized through a typical mass–damper–spring (MDS) system attached at the right-hand side boundary of the moving string. The dynamic coupling between the string and the MDS system provides an actuation force to suppress transverse vibration. In the first phase of this study, the framework of FSMC is designed, in which the techniques of region-wise linear fuzzy logic control design and generic algorithm technique are employed to facilitate FSMC to reduce a large number of fuzzy rule bases and to select optimal control gains, respectively. In the second phase, the FNNC is developed, which is, compared to the FSMC, easier to design the control rule, more robust against environment and capable of on-line learning. Numerical simulations are conducted and the comparison between various controllers is made based on simulations. The simulated results show that the transverse vibration can be well suppressed by both approaches. FSMC offers the capability to regulate the transient response, while FNNC holds advantage of on-line learning capability.

1. Introduction

The axially moving string system can be applied to many mechanical systems such as cable tramways, band saws, fiber winders, fluid pipes, magnetic tapes, traveling strings and power transmission chains/belts. Carrier [1] proposed an approximate non-linear theory to describe the vibration of a string. Mote [2], Wickert and Mote [3,4], and Lee and Mote [5] analyzed stability, vibration and energetics of the axially moving system. Chen [6] studied the natural frequencies

*Corresponding author. Fax: +886-3-265-4399.
E-mail address: pchao@cycu.edu.tw (P.C.-P. Chao).

0022-460X/03/$ - see front matter
doi:10.1016/S0022-460X(02)01082-9

and stability of the axially moving string in contact with a stationary load system. In this study, the effects of system parameters such as dry friction, inertia, damping and stiffness were also investigated on the stability and nature frequency of the system.

Boundary control is an economic approach to control distributed parameter systems (DPS) due to the reason that it does not need sensors or actuators attached to the main body of controlled continuous system. Furthermore, active and passive controls can be easily implemented at boundaries. As results, this "boundary control" becomes a popular research topic recently. Chen [7] estimated the energy decay of a wave equation in a bounded domain. Jai and Pritchard [8] found that if sensors or actuators located at nodal points, the DPS is uncontrollable and unobservable. Yang and Mote [9], Chung and Tan [10], and Yang and Mote [9] performed s-domain analysis. Chung and Tan [10] proposed active vibration control implemented by wave cancellation. Lee and Mote [11] used the boundary controller to suppress vibration of an axially moving string. Fung and Tseng [12] designed a new boundary controller by the method of sliding-mode control via Lyapunov function formulation. The asymptotic stability of this controlled system is proved by semi-group theory. However, the control effort generated becomes unbounded as the trajectory approaches origin.

A number of researchers investigated the relationship between sliding-mode and fuzzy control. Palm [13] proposed a specific class of fuzzy controllers derived from the phase plane, which is similar to the sliding-mode control with a boundary layer. Yager and Filev [14] determined the fuzzy rules according to the sliding-mode condition. Lu and Chen [15] combined the best features of self-organizing fuzzy control and sliding-mode control to achieve rapid and accurate tracking control of a class of non-linear systems. The fuzzy rule base is used to approximate the equivalent control through self-organizing, and the variable structure control effort is used to compensate for the approximation error and to provide exponential convergence of the sliding variable. Wu and Liu [16] used the sliding modes to determine the best values for the parameters in the fuzzy control rules to improve robustness of fuzzy control. The Lyapunov function and the boundary layer have been employed in this study to satisfy the reaching condition and to avoid chattering, respectively. Fung et al. [17] designed a region-wise linear fuzzy sliding-mode controller to regulate toggle and quick-return mechanism.

There have been considerable interests in the past few years for exploring the applications of fuzzy neural network (FNN) systems, which combine the capability of fuzzy reasoning to handle uncertain information [14,18–20] and that of artificial neural networks to learn from processes [21–24]. This approach would be able to deal with non-linearities and uncertainties of control systems [20,25–30]. For instance, the adaptive fuzzy systems or FNNs are introduced as identifiers for non-linear dynamic systems based on the back-propagation algorithm [19]. Chen and Teng [28] proposed a model reference control structure using an FNN controller, which is trained on-line through an FNN identifier with adaptive learning rates. Zhang and Morris [29] provided a technique for modelling of non-linear systems using an FNN topology. Jang and Sun [30] reviewed the advances in neuro-fuzzy synergisms for modelling and control based on the framework of adaptive network.

This study is aimed to suppress transverse vibration of an axially moving string by application of a mass–damper–spring system (MDS) at the RHS of the axially moving string system. Two general types of fuzzy control schemes are employed to seek out the successes of intelligent control schemes. The first type utilizes pre-defined sliding function and its derivatives as the input

variables for the fuzzy system to determine the ensuing fuzzy logics—mimicking the approach in the conventional sliding-mode control. Therefore, this control scheme is named as "fuzzy sliding-mode control" (FSMC) as in Refs. [16,17]. This control design resolves two common difficulties of initializing a fuzzy control design: (1) The synthesis process of fuzzy control logics is often experience oriented such that a great difficulty exists for designers to establish fuzzy rule bases, and (2) For most cases, little knowledge is available for the system characteristics. In addition to the above two advantages for design, the FSMC forces the system dynamics first converge to the sliding surface before reaching the origin, providing the means to regulate the transient response. To reduce the number of fuzzy rule bases and to select the optimal control gains, respectively, the techniques of region-wise linear fuzzy logic control (RLFLC) and generic algorithm (GA) can be employed to assist the FSMC. The second type of approaches is the fuzzy neural network control (FNNC), which utilizes neural networks to perform an on-line learning of the system dynamics and to synthesize fuzzy reasonings to handle system uncertainty [14,18–20]. It would be found based on the design process and simulation of the controlled systems that FSMC has ability to regulate the system transient response through the sliding function formulation and easy to build, while FNNC holds the capability of robust and on-line learning. Compared to the boundary control for the axially moving string system via sliding-mode control adopted by Fung and Tseng [12], FSMC and FNNC proposed herein both hold capability of tackling parametric uncertainty and generating bounded control efforts, which renders application realizable.

2. Equations of motion

The physical model of an axially moving string system is depicted in Fig. 1. A moving string passes through one fixed end and a mass–damper–spring (MDS) system acts at the other end. The MDS includes a lump mass m, a viscous damper with constant coefficient d_m and a spring with constant stiffness k_m. The string spans in total length of l, the mass per unit length of which is ρ, the material damping is denoted by c_v, and the axially rigidity of the string EA. The string is assumed subjected to an initial tension force T_0 and move axially in a constant translating speed c. The string exhibits the transverse displacement v at axial co-ordinate x. The control actuation input f_c is applied at the mass of a mass–damper system attached at the RHS of the string for the purpose of suppressing the transverse oscillations. The dimensionless governing equation and boundary conditions of the axially moving string system [12] are

$$V_{\tau\tau} + \eta_v(V_\tau + \beta V_\xi) + 2\beta V_{\xi\tau} + (\beta^2 - 1)V_{\xi\xi} - \tfrac{3}{2}\beta_1^2 V_\xi^2 V_{\xi\xi} = 0, \tag{1a}$$

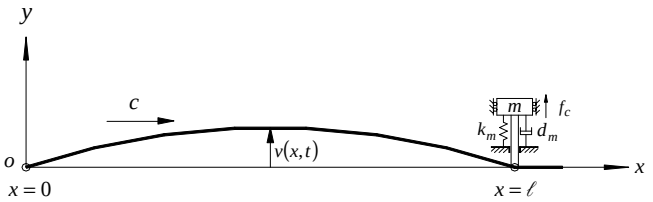

Fig. 1. An axially moving string system with MDS controller.

$$V(0,\tau)=0, \tag{1b}$$

$$F_c = q_{\tau\tau} + (\eta_m - m_r\beta)q_\tau + S_m q - m_r(\beta^2 - T_{s1})q_1, \tag{1c}$$

where

$$V=\frac{v}{l}, \quad \xi=\frac{x}{l}, \quad \tau=\frac{C_2 t}{l},$$

$$q(\tau)=V(l,\tau), \quad q_\tau(\tau)=V_\tau(l,\tau), \quad q_{\tau\tau}(\tau)=V_{\tau\tau}(l,\tau),$$

$$q_1(\tau)=V_\xi(l,\tau), \quad T_{s1}=1+\tfrac{1}{2}\beta_1^2 q_1^2,$$

$$C_1=\sqrt{\frac{EA}{\rho}}, \quad C_2=\sqrt{\frac{T_0}{\rho}}, \quad \beta=\frac{c}{C_2}, \quad \beta_1=\frac{C_1}{C_2},$$

$$\eta_v=\frac{c_v l}{\rho C_2}, \quad \eta_m=\frac{d_m l}{m C_2}, \quad F_c=\frac{f_c l}{m C_2}, \quad S_m=\frac{k_m l^2}{m C_2^2}, \quad m_r=\frac{\rho l}{m}.$$

Note in Eq. (1) that the subscripts with respect to V and q are temporal differentiations except for the notation q_1, τ is the non-dimensionalized quantity of time t. The last term in Eq. (1a) characterizes the geometric non-linearity. f_c is the actuation force exerted by the MDS and F_c is the associated non-dimensionalized counterpart. With the governing equations in hand, the dimensionless form of the total mechanical energy is then

$$\tilde{E}(\tau)=\frac{1}{2}\int_0^l (V_\tau+\beta V_\xi)^2\,\mathrm{d}\xi+\frac{1}{2}\int_0^l V_\xi^2\,\mathrm{d}\xi+\frac{1}{8}\beta_1^2\int_0^l V_\xi^4\,\mathrm{d}\xi+\frac{1}{2}\bar{m}_r(q_\tau^2+S_m q^2), \tag{2}$$

where $\bar{m}_r=1/m_r$. Note from Eqs. (1) and (2) that the condition $\beta_1=0$ reduces Eqs. (1) and (2) to linear equations.

3. Fuzzy sliding-mode control

In recent years, there have been many successful applications using fuzzy control and sliding-mode control, but there still exist several difficulties. First, the establishment of fuzzy control rules is model dependent and experience oriented. Second, to render smooth control response, the number of rule bases rises exponentially, which increase level of design difficulty. Third, it needs effort to find suitable shapes for membership functions. To remedy the aforementioned problems, some techniques are applied. The first one is the fuzzy logic control plus sliding-mode formulation, which reduce the size of the computations consumed by fuzzy reasoning. The second one is the technique of RLFLC scheme applied to fuzzy logics, which reduces the number of fuzzy rules. The third one is the GA, which could help find optimal membership functions that generate a control within prescribed saturation bounds for fast responses.

3.1. Design of the fuzzy sliding-mode control

To initialize FSMC design, the sliding-mode formulation is adopted to establish the fuzzy logic rules. First, the sliding function, denoted by s, captures the sum of displacement and velocity of the oscillating string at RHS boundary; i.e., $s \equiv e + \dot{e}$ where $e = V(l, \tau)$ plays the role of the conventional error function for fuzzy control design, which is desired to be suppressed. In this way, the FSMC designed is capable of first converging the system dynamics to the neighborhood of the sliding surface before reaching the origin; in other words, providing the means to regulate the transient response. In practice and ensuing simulation, $\dot{e}$ and $\dot{s}$ are considered available by the discrete approximation of

$$\dot{e}(KT) = \frac{1}{T}[e(KT) - e(K-1)T],$$

$$\dot{s}(KT) = \frac{1}{T}[s(KT) - s(K-1)T], \tag{3}$$

where K is the number of iteration and T is the sampling period. The output of the FSMC is F_c, the actuation force on the MDS. In order to accommodate various system characteristics for a better control, the sliding functions s and $\dot{s}$ are multiplied by scaling factors G_S and G_{CS}, respectively. These factors are mainly used to equip designers with the capability of adjusting control gains before s and $\dot{s}$ taken as inputs for membership functions. The scalings give

$$S = sG_S, \quad \dot{S} = \dot{s}G_{CS}. \tag{4}$$

The associated fuzzy sets are determined as follows:

N: Negative,	Z: Zero,	P: Positive,
NH: Negative huge,	NB: Negative big,	NM: Negative medium,
NS: Negative small,	ZE: Zero,	PS: Positive small,
PM: Positive medium,	PB: Positive big,	PH: Positive huge.

The membership functions for the fuzzy sets of S, $\dot{S}$ and F_c are defined and illustrated in Fig. 2. It is seen from this figure that only five fuzzy subsets, NB, NM, Z, PM, PB, are defined for S and $\dot{S}$, which require subsequently 25 fuzzy rules to accomplish the fuzzy control design. The resulting fuzzy sliding-mode inference rules are shown in Table 1, where F_c is the fuzzy mapped function of S and $\dot{S}$. Note that the essence of rules in Table 1 originates from the concept of the conventional feedback control in which F_c plays the role of negative feedback. Note also that by imposing the upper/lower bounds on the membership function of F_c, one is able to realize the actual saturation of the control effort, which is often difficult for most conventional control design approach.

3.2. Design of region-wise linear fuzzy logic control

As the number of input variables for fuzzy controller increases, the number of fuzzy if–then rules increases exponentially; consequently, this increases a great deal of computation burden to synthesize fuzzy control output. In order to minimize the effort of control synthesis, the technique region-wise linear fuzzy control is applied herein to FSMC. The controller equipped with this technique is named RLFLC.

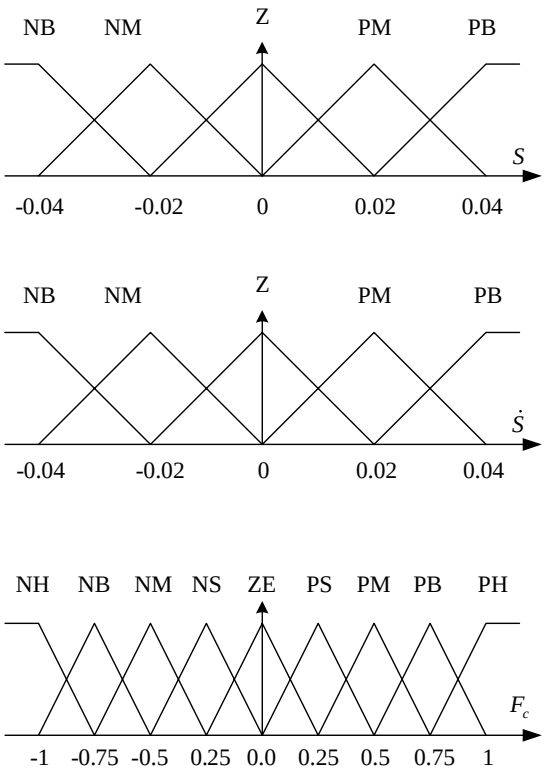

Fig. 2. Membership functions for the fuzzy sets corresponding to S, $\dot{S}$ and F_c.

Table 1
Linguistic rules based on FLC for the axially moving string system

F_c		$\dot{S}$				
		NB	NM	Z	PM	PB
S	NB	PH	PB	PM	PS	ZE
	NM	PB	PM	PS	ZE	NS
	Z	PM	PS	ZE	NS	NM
	PM	PS	ZE	NS	NM	NB
	PB	ZE	NS	NM	NB	NH

For implementing the region-wise technique, a region-wise functions S^* is first defined as

$$S^* = S + \dot{S}. \tag{5}$$

Table 2 lists the fuzzy relationship among S^*, S and $\dot{S}$, where the fuzzy variable S^* characterizes the sum effect of S and $\dot{S}$. The information revealed in both Tables 1 and 2 makes possible the derivation of the fuzzy relationship between F_c and S^* which is listed in Table 3. The variable S^* is now considered the new sole fuzzy variable to synthesize fuzzy controller. The corresponding memberships designed for S^* and F_c are given in Fig. 3. Compared to the original scheme of

Table 2
Relationships between S^*, S and $\dot{S}$ for the axially moving string system

S^*		$\dot{S}$				
		NB	NM	Z	PM	PB
S	NB	NH	NB	NM	NS	ZE
	NM	NB	NM	NS	ZE	NS
	Z	NM	NS	ZE	PS	PM
	PM	NS	ZE	PS	PM	PB
	PB	ZE	PS	PM	PB	PH

Table 3
Rule base for RLFLC

S^*	PH	PB	PM	PS	ZE	NS	NM	NB	NH
F_c	NH	NB	NM	NS	ZE	PS	PM	PB	PH

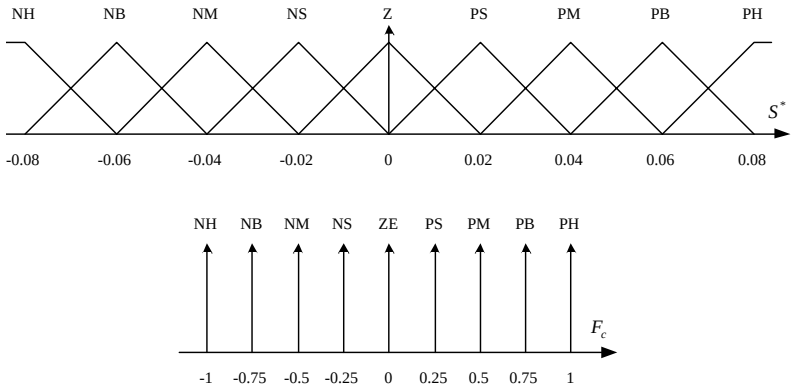

Fig. 3. Membership functions of S^* and F_c for RLFLC.

FSMC, this method of RLFLC reduces the number of fuzzy variable from two (S and $\dot{S}$) to one (S^*); as result, decreasing greatly the number of fuzzy linguistic rules. Note, however, that the dynamic characteristics of the RLFLC are not different from FSMC in nature.

3.3. Genetic algorithm (GA) for scaling factor design

The scaling factors G_S and G_{CS} in Eq. (4) allow designers to perform control tunings through re-shaping of membership functions. It is expected to result in a better performance in terms of overshoot, response time, etc. Large values of G_S and G_{CS} generally render an effect of large control gains, which may causes small rise time and chattering, while small G_S and G_{CS} may lead to long settling time or even destabilizing system. The Genetic Algorithm is a numerical algorithm used to find optimal shapes of membership functions via minimizing a prescribed cost function

that makes design objective probable. This cost function is the so-called fitness function F, defined by

$$F = \frac{1}{J+1}, \tag{6a}$$

where the objective function J is the discrete sum of displacement at the middle point of the string times the sampling time; i.e.,

$$J = \sum |V(l/2, \tau)\Delta\tau|, \tag{6b}$$

where $\Delta\tau$ is the sampling time. With the fitness function defined, one is able to find optimal values of G_S and G_{CS} numerically [31]. Note that since the mid-point vibration level, $V(l/2, \tau)$ in J given in Eq. (6b), are not often measurable, the optimal values of G_S and G_{CS} would be obtained off-line through an optimization process based on a fitness function Eq. (6a). This process demands a high accuracy of mathematical model to ensure the effectiveness of FSMC controller. To avoid this drawback of GA, the method of neural network will be employed to realize on-line learning of model in the ensuing study.

4. Design of the FNNC

4.1. Fuzzy neural network

A general four-layer FNN structure shown in Fig. 4 is adopted to implement the proposed FNN controller, which consists of the input (i layer), membership (j layer), rule (k layer), and output (o layer) layers. The signals e and $\dot{e}$ in Fig. 4 are error input for the FNN mechanism and its time derivative, respectively. e is defined by $e = q(\tau) - q_d$, where $q(\tau)$, as given previously in Eq. (1), is the displacement at RHS of the oscillating string and q_d is the desired value of $q(\tau)$ at

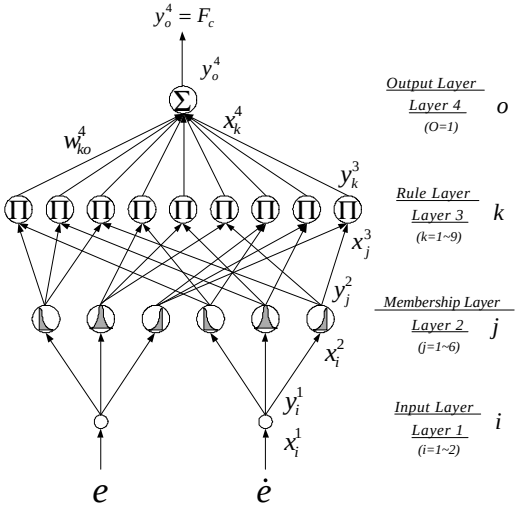

Fig. 4. Structure of the four-layer FNN.

steady state, which is set to be zero for satisfactory vibration suppression. The output of the FNN would be used for realizing the actuation of the MDS; i.e., F_c. The nodes in the input layer represent the input linguistic variables. Those in the membership layer act as the membership functions. Moreover, all the nodes in the rule layer represent a fuzzy rule base. The signal propagation and the basic function of each layer are elaborated in the following:

4.1.1. Layer 1: (input layer)

For every node i in this layer, the net input and the net output are related by

$$net_i^1 = x_i^1, \quad y_i^1 = f_i^1(net_i^1) = net_i^1, \quad i = 1, 2, \tag{7}$$

where x_i^1 represents the ith input to the node of layer 1.

4.1.2. Layer 2: (membership layer)

In this layer, each node plays a role of a membership function. The Gaussian function is adopted as the membership function. For the jth node

$$net_j^2 = -\frac{(x_i^2 - m_{ij})^2}{(\sigma_{ij})^2},$$

$$y_j^2 = f_j^2(net_j^2) = \exp(net_j^2), \quad i = 1, 2, \quad j = 1 \sim 6, \tag{8}$$

where m_{ij} and σ_{ij} are, respectively, the mean and the standard deviation of the Gaussian function for the jth node, which takes the ith linguistic variable x_i^2 as the input. Note that the main objective of the layer 2 is to form the membership functions for incorporating the fuzzy logics in the structure of neural network; therefore, the weights between layers 1 and 2 are set as unities, bearing no responsibility of updating. As result, in Fig. 4, the weights between layers 1 and 2 are not denoted.

4.1.3. Layer 3: (rule layer)

Each node k in this layer is denoted by Π, which multiplies the incoming signal with weightings and outputs the resulted product. For the kth rule node,

$$net_k^3 = \prod_j w_{jk}^3 x_j^3, \quad y_k^3 = f_k^3(net_k^3) = net_k^3, \quad j = 1 \sim 6, \quad k = 1 \sim 9, \tag{9}$$

where x_j^3 represents the jth input to the node of layer 3. The weights between layers 2 and 3 are also set to be unities herein, leaving the adaptation capability of this FNN scheme, shaping on membership functions and adjusting weightings, to be performed in layer four.

4.1.4. Layer 4: (output layer)

The single node o in this layer is a labelled by Σ, which computes the overall output by summing all incoming signals as

$$net_o^4 = \sum_k w_{ko}^4 x_k^4, \quad y_o^4 = f_o^4(net_o^4) = net_o^4, \quad o = 1, \tag{10}$$

where the link weights w_{ko}^4's are the output action strength of the oth output associated with the kth rule; x_k^4 represents the kth input to the node of layer 4, y_o^4 is the output of the neural network. In practice, y_o^4 is realized by the actuation of the MDS; i.e., $y_o^4 = F_c$.

4.2. On-line learning algorithm using delta adaptation law

The key part of the learning algorithm for the FNN is how to recursively obtain a gradient vector in which each element in the learning algorithm is defined as the derivative of a performance function with respect to a design parameter of the network. This is done by means of the chain rule, and the method is generally referred to as the back-propagation learning rule because the gradient vector is calculated in the direction opposite to the flow of the output of each node [26]. To describe the on-line learning algorithm of the FNN, the performance function $P(\tau)$ for the system of axially moving string is first defined as

$$P(\tau) = \tfrac{1}{2}(q(\tau) - q_d)^2 = \tfrac{1}{2}e^2, \tag{11}$$

where e, based on the definitions of $q(\tau)$ given previously in Eq. (1), represents the difference between the displacement at RHS of the oscillating string and the desired one q_d. Note that $q(\tau)$ is the feedback signal and q_d is set to be zero for maximum vibration suppression of the string. With the performance function (11) defined, the learning algorithm based on the back-propagation is next formulated by the update laws for each layer, which are stated as follows in a backward fashion.

4.2.1. Layer 4

The error term to be propagated is given by

$$\delta_o^4 = -\frac{\partial P}{\partial y_o^4} = \left[-\frac{\partial P}{\partial e}\frac{\partial e}{\partial y_o^4}\right] = \left[-\frac{\partial P}{\partial e}\frac{\partial e}{\partial q}\frac{\partial q}{\partial y_o^4}\right] \tag{12}$$

and the weights are updated by

$$\Delta w_{ko}^4 = -\eta_w \frac{\partial P}{\partial w_{ko}^4} = \left[-\eta_w \frac{\partial P}{\partial y_o^4}\right]\left(\frac{\partial y_o^4}{\partial net_o^4}\frac{\partial net_o^4}{\partial w_{ko}^4}\right) = \eta_w \delta_o^4 x_k^4, \tag{13}$$

where the factor η_w is the learning-rate parameter of the weight. The weights of the output layer are updated according to the following equation:

$$w_{ko}^4(N+1) = w_{ko}^4(N) + \Delta w_{ko}^4, \tag{14}$$

where N denotes the iteration number, while the initial values of weights are set to be uniform over the output space of layer 3 for simplicity.

4.2.2. Layer 3

In this layer since the weights were set to be unities, only the error terms need to be calculated and propagated, yielding

$$\delta_k^3 = -\frac{\partial P}{\partial net_k^3} = \left[-\frac{\partial P}{\partial y_o^4}\right]\left(\frac{\partial y_o^4}{\partial net_o^4}\frac{\partial net_o^4}{\partial y_k^3}\frac{\partial y_k^3}{\partial net_k^3}\right) = \delta_o^4 w_{ko}^4. \tag{15}$$

4.2.3. Layer 2

The multiplication operation is performed in this layer

$$\delta_j^2 = -\frac{\partial P}{\partial net_j^2} = \left[-\frac{\partial P}{\partial y_o^4}\frac{\partial y_o^4}{\partial net_o^4}\frac{\partial net_o^4}{\partial y_k^3}\frac{\partial y_k^3}{\partial net_k^3}\right]\left[\frac{\partial net_k^3}{\partial y_j^2}\frac{\partial y_j^2}{\partial net_j^2}\right] = \sum_k \delta_k^3 y_k^3. \tag{16}$$

The update law of m_{ij} is

$$\Delta m_{ij} = -\eta_m \frac{\partial P}{\partial m_{ij}} = \left[-\eta_m \frac{\partial P}{\partial y_j^2}\frac{\partial y_j^2}{\partial net_j^2}\frac{\partial net_j^2}{\partial m_{ij}}\right] = \eta_m \delta_j^2 \frac{2(x_i^2 - m_{ij})}{(\sigma_{ij})^2} \tag{17}$$

and the update law of σ_{ij} is

$$\Delta\sigma_{ij} = -\eta_\sigma \frac{\partial P}{\partial \sigma_{ij}} = \left[-\eta_\sigma \frac{\partial P}{\partial y_j^2}\frac{\partial y_j^2}{\partial net_j^2}\frac{\partial net_j^2}{\partial \sigma_{ij}}\right] = \eta_\sigma \delta_j^2 \frac{2(x_i^2 - m_{ij})^2}{(\sigma_{ij})^3}. \tag{18}$$

The mean and standard deviation of the membership function layer are updated as follows:

$$m_{ij}(N+1) = m_{ij}(N) + \Delta m_{ij}, \tag{19}$$

$$\sigma_{ij}(N+1) = \sigma_{ij}(N) + \Delta\sigma_{ij}. \tag{20}$$

Recall that m_{ij}'s and σ_{ij}'s are, respectively, the mean and the standard deviation of the Gaussian membership functions employed. The factor η_m's and η_σ's are the learning-rate parameters of the mean and the standard deviation of the Gaussian function, respectively.

Note that while computing Eq. (12), the update law in the layer 4, the Jacobian of the system at RHS of Eq. (12); i.e., $\partial q/\partial y_o^4$, cannot be determined directly due to the unknown dynamics of the control system. Although an additional FNN identifier can be utilized to solve the problem, ensuing heavy computation efforts are required to complete the calculation involved in layers 1 and 2. In order to ease computation and to increase the on-line learning rate of the weights, a delta adaptation law for simplifying Eq. (12) is proposed as follows [32]:

$$\delta_o^4 \cong C_{FNN} e + \dot{e}, \tag{21}$$

where C_{FNN} is a positive constant coefficient used to tune the degree of the relative emphases on e and $\dot{e}$. Note that with pre-determined C_{FNN} Eq. (21) allows us to skip the complicated computation of Eq. (12). Based on common practice, larger gains of C_{FNN} cause a faster convergence, but may destabilize the controlled system.

5. Numerical results

The finite difference approach is used herein to discretize the governing PDE (1) and numerically simulate the response of the system. To conduct finite difference analysis, the total length of the string is first discretized into N sections in equal section lengths $\Delta\xi$'s, and the

temporal axis is also discretized by $\Delta\tau$. The explicit central difference algorithm is adopted with the choice of spatial discretization parameter $N = 20$. The stability for the convergence of the finite difference criterion is [33]

$$\Delta\tau \leqslant \frac{\Delta\xi^2}{2}. \tag{22}$$

With $N = 20$ and $l = 1$ (since l is already normalized) $\Delta\xi$ is equal to $\Delta\xi = l/N = 0.05$. Also, the temporal axis is discretized by $\Delta\tau = 0.00125$. The determined $\Delta\xi$ and $\Delta\tau$ lead to $\Delta\tau/\Delta\xi^2 = 0.5$, which satisfies the convergence criterion (22).

The dimensionless parameters for the string and the MDS are considered as $l_0 = 1\,\text{m}$, $T_0 = 40\,\text{N}$, $\eta_v = 0$, $C_1 = 63.25$, $C_2 = 6.33$, $\beta = 0.02$, $\beta_1 = 10$, $m_r = 2$, $S_m = 1$ and $\eta_m = 0.32$. The initial shape of the transverse displacement of the string is given by $V(\xi, 0) = 0.05\xi$. The ranges of G_S and G_{CS} are set to be $0 < G_S \leqslant 3.1$ and $0 < G_{CS} \leqslant 3.1$ for optimization.

In practice, the tension T_0 and total length l of the axially moving string varied slightly while the string is in vibration. The associated variations on T_0 and l are considered as parametric variations and external load disturbance, respectively, by

Parameter variation:

$$l(\tau) = l + 0.06 * |q(\tau)|, \tag{23}$$

$$T(\tau) = T_o + 40 * |q(\tau)|. \tag{24}$$

External disturbance:

$$q_{dis} = 6 \times 10^{-4} \text{ occur only at } \tau = 5. \tag{25}$$

Note that the disturbance for T_0 and l in Eqs. (23) and (24) are set to be proportional to oscillating displacement at RHS of the string, which reflects the geometric and physical reality. The disturbance in Eq. (25) is set to be in a form of displacement disturbance with a small value of $q_{dis} = 6 \times 10^{-4}$ occurring at $\tau = 5$.

Fig. 5 shows the simulation results for the case in which the FSMC is applied without the assistance from the GA technique. Note that herein due to prior non-dimensionalizations performed on the governing Eqs. (1) for all system variables, in this figure where simulation results are shown, as well as Figs. 6–8 presented later, all physical quantities corresponding to x- and y-axis are dimensionless (including time). In Fig. 5, four different cases are conducted and presented: an uncontrolled system (dotted curves), the uncontrolled system with parameter variations prescribed by Eqs. (23) and (24) (dot–dashed curves), a controlled system (dashed curves) and the controlled system subjected to external disturbance prescribed by Eq. (25) (solid curves). Figs. 5(a) and (b) show the displacements at middle point ($l = \frac{1}{2}$) and the RHS boundary ($l = 1$) of the axially moving string, respectively. Fig. 5(c) shows the time history of total mechanical energy defined by Eq. (2). Note that herein the spatial integration for computing Eq. (2) is approximated by the trapezoidal integration method. Fig. 5(d) shows the phase-plane of the RHS boundary oscillation, where it is seen that the state trajectory approach the $s = 0$ subspace as the FSMC is employed. Fig. 5(e) shows the corresponding control effort. Note that the external disturbance prescribed by Eq. (25) is applied to the RHS of the string system at $\tau = 5$ for testing the capability of disturbance rejection by the controllers. It is seen from Figs. 5(a)–(d) that the transverse vibration of the controlled systems is well suppressed by the FSMC as compared to those

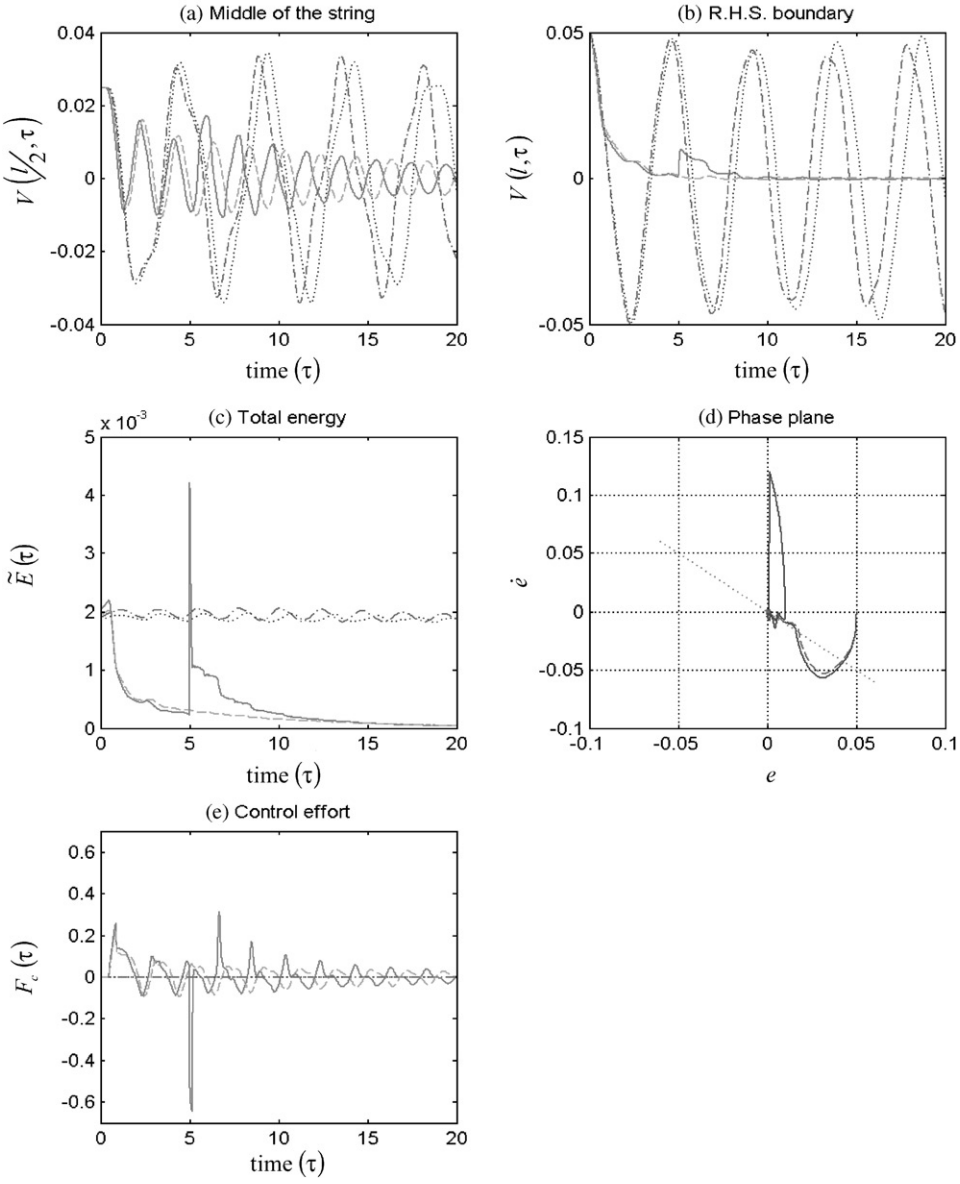

Fig. 5. Boundary control of the axially moving string system via FSMC method: (a) the transverse vibrating amplitudes at the midpoint of the system, (b) the transverse amplitudes at the RHS boundary of the system, (c) the total energy of the control system, (d) the phase plane, (e) the control effort. "…", Uncontrolled system; "–·", uncontrolled system with parameter variations; "––", controlled system and "–", the controlled system subjected to external disturbance prescribed.

uncontrolled; moreover, a good rejection of disturbance is achieved by the FSMC even though finite spikes are present around $\tau = 5$, as shown by the case denoted by solid curves.

In order to obtain a better vibration suppression at midpoint, the optimal scaling factors G_S and G_{CS} in Eq. (4) are searched via the GA technique to assist the FSMC controller. The related

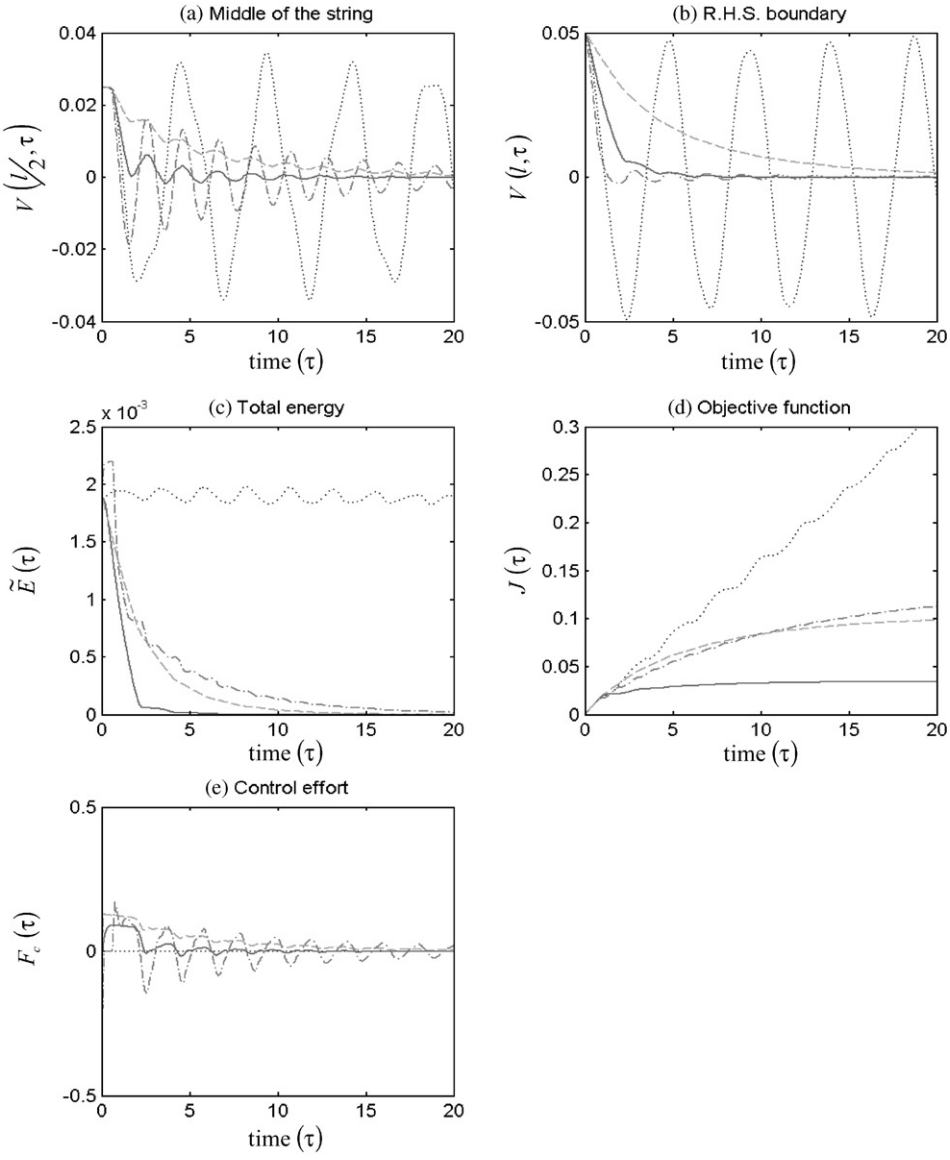

Fig. 6. Boundary control of the axially moving string system via FSMC assisted by GA method: (a) the transverse amplitudes at the midpoint of the system, (b) the transverse amplitudes at the RHS boundary of the system, (c) the total energy of the control system, (d) the objective function, (e) the control effort. "…", Uncontrolled system; "–·", controlled system with $(G_S, G_{CS}) = (1.9, 0.9)$; "––", $(G_S, G_{CS}) = (0.1, 1.8)$ and "–", the controlled system with optimal gain $(G_S, G_{CS}) = (0.1, 0.5)$.

procedure of computation was stated in Section 3.3. Figs. 6(a)–(d) shows the simulation results where the dotted curves represent the uncontrolled case, the solid curves represent the controlled case with optimized $(G_S, G_{CS}) = (0.1, 0.5)$ by GA technique, and the dot–dashed and dashed

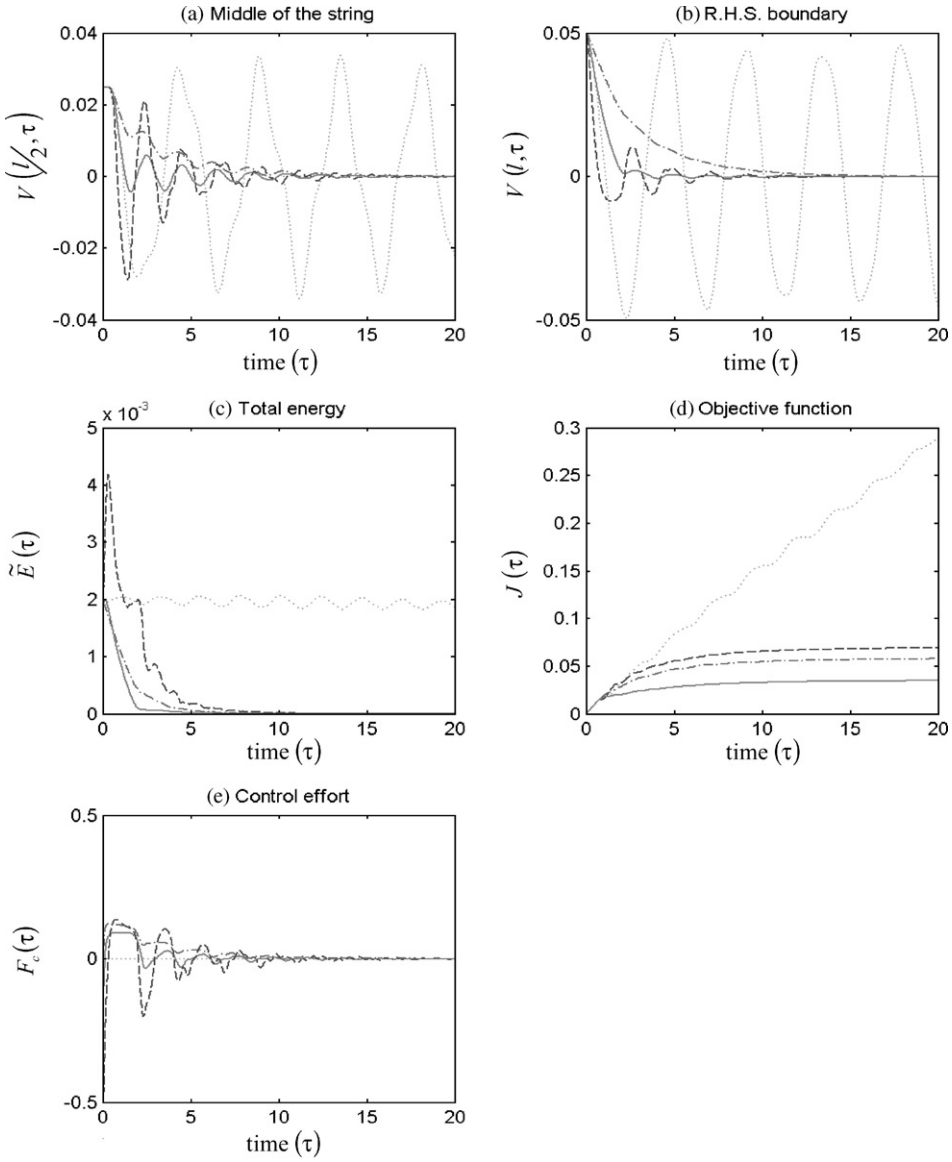

Fig. 7. Boundary control of the axially moving string system via RLFLC assisted by GA: (a) the transverse amplitudes at the midpoint of the system, (b) the transverse amplitudes at the RHS boundary of the system, (c) the total energy of the control system, (d) the objective function, (e) the control effort. "…", Uncontrolled system; "–·", controlled system with $(G_S, G_{CS}) = (1.9, 0.9)$; "––", $(G_S, G_{CS}) = (0.1, 1.8)$ and "–", the controlled system with optimal gain $(G_S, G_{CS}) = (0.3, 0.5)$.

curves correspond to those with $(G_S, G_{CS}) = (1.9, 0.9)$ and $(G_S, G_{CS}) = (0.1, 1.8)$, respectively. Note that the total mechanical energy shown in Fig. 6(c) and the objective function given by Eq. (6) in Fig. 6(d), enable the performance evaluation on the controllers. Fig. 6(e) shows the

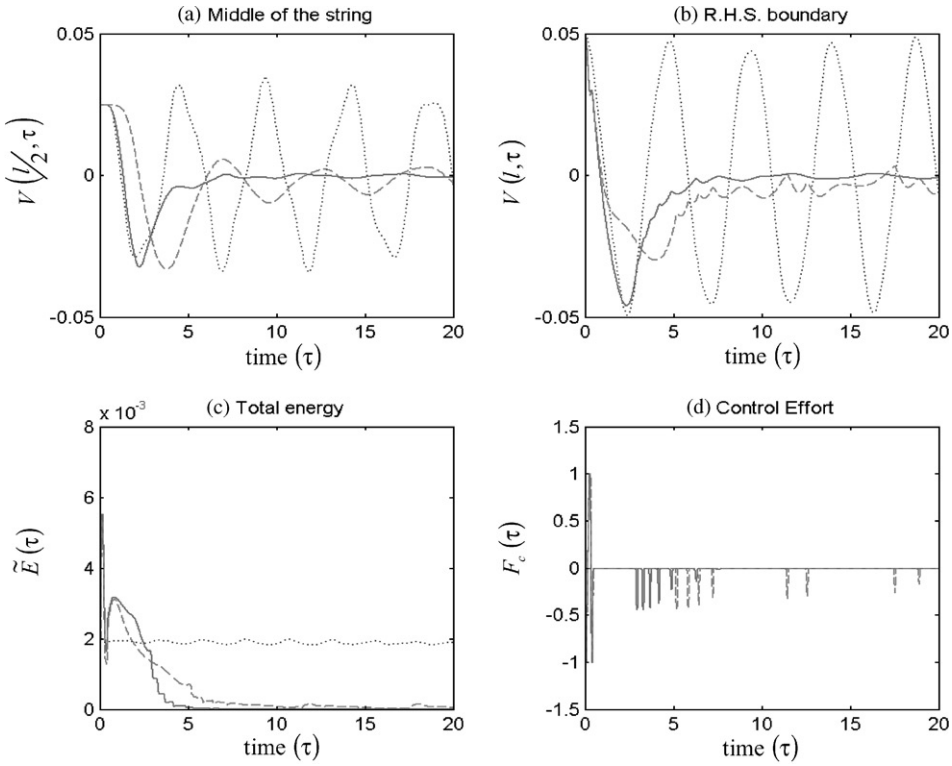

Fig. 8. Boundary control of the axially moving string system via FNNC: (a) the transverse amplitudes at the midpoint of the system, (b) the transverse amplitudes at the RHS boundary of the system, (c) the total energy of the control system, (d) the control effort. "…", Uncontrolled system; "––", controlled system with small gain $C_{FNN} = 0.2$ and "–", the controlled system with large gain $C_{FNN} = 0.5$.

control effort. It is seen from these figures that the optimized (G_S, G_{CS}) obtained by the GA technique renders faster vibration suppression and smoother system response of string.

Fig. 7 shows the simulated results using the design schemes of RLFLC equipped with the technique of GA where the dotted curves represent the uncontrolled case. Solid curves represent the results with the optimized $(G_S, G_{CS}) = (0.3, 0.5)$ applied, while dashed and dot–dashed curves represent the cases with $(G_S, G_{CS}) = (0.1, 1.8)$ and $(G_S, G_{CS}) = (1.9, 0.9)$, respectively. It is seen from these figures that as compared to the simulated results of FSMC with GA shown in Figs. 6, a reduction of rule bases by RLFLC renders a similar general characteristic of controller performance. This is due to the fact that RLFLC only provides a simplified computation technique of the fuzzy logics rather than change dynamic nature of the controllers.

Fig. 8 shows the simulated results using the FNN control scheme. Dotted curves represent the uncontrolled case while dashed and solid curves show the controlled results with $C_{FNN} = 0.2$ and 0.5, respectively. It is seen from the figures that the larger gains are used, the faster decay of string transverse vibration is obtained either at RHS boundary or midpoint of the moving string.

6. Discussions

Some conclusive remarks about various control designs based on controller development, analysis and simulations are pertinent at this point.

- The merit of sliding function formulations for the fuzzy logics control as used for FSMC is clearly demonstrated in Fig. 5(d), where it can be seen that the state trajectory approaches the sliding surface initially and then follow it to the origin. This provides the designer a tool to regulate the transient response and simultaneously guarantee the ultimate convergent tendency to the origin; i.e., in physical sense, reduce the transverse vibration substantially.
- A general comparison in terms of transient and steady state responses between Figs. 5(a), (b), 6(a) and (b) shows that the FSMC with off-line optimized GA technique renders much better transverse vibration reductions than the sole FSMC either at midpoint or RHS boundary of the moving string. This result strongly recommends the usage of the GA technique to tune the FSMC. However, the demonstrated controller performance by the FSMC with optimized GA gains would be only possibly achieved by the off-line simulations/computations based on an accurate established mathematical model.
- In order to overcome the disadvantage of the off-line tuning by the FSMC with optimized GA gains, the FNNC is recommended consequently in this study. The neural network adopted in the framework of FNNC is able to search for better membership functions of the fuzzy logic rules for the purpose of tuning the controller in an on-line fashion.
- Both control designs of FSMC/RLFLC and FNNC possess the merit of robustness due to the fact that the information of mathematical model is not required for controller synthesis and activation.
- All control designs proposed, FSMC/RLFLC, FSMC with GA and FNNC, provide the option to impose a limitation on the control effort through the fuzzy output formulation, which complies with most actuators' realistic specification. This holds the advantage over the approach recommended by Fung and Tseng [12], where the large control efforts were generated.
- Conclusively speaking, the proposed control design schemes suit for different goals and scenarios. The FSMC/RLFLC provides the access to manage the transient response based on the fuzzy inputs derived from the formulations of sliding functions. The FSMC with GA provides the tool of tuning the FSMC based on the mathematical model to find optimum scalings; however, any inaccuracy in the mathematical model would deteriorate the control design; i.e., no robustness is guaranteed. The FNNC offers an automatic on-line tuning control scheme only based on the input–output characteristics; however, the updating process of the neural network adopted may result in a longer time for the system to converge.

7. Conclusions

This study successfully proposed various intelligent fuzzy control schemes to perform boundary control of the axially moving string system for the purpose of transverse vibration reduction. The control schemes are mainly FSMC/RLFLC, FSMC with GA and FNNC. In the framework of

FSMC/RLFLC, the sliding function is employed as fuzzy inputs to provide the capability for the designer to regulate the transient response of the system. The scheme of FSMC with GA offers a off-line computation procedure to optimize the scalings on the fuzzy inputs of the sliding functions in order to search the faster/smoother vibration reduction. Due to possible inaccuracy resided in the mathematical model obtained, an on-line tuning approach, FNNC is proposed to perform transverse vibration reduction, in which the weights in the structure of the neural network are actively updated to reach to a best-tuned controller. The FSMC/RLFLC provide advantages of regulated transient response and robustness. The FSMC with GA makes possible the FSMC tuning based on the mathematical model with the price of losing robustness. The FNNC offers an on-line tuning control scheme; however, without experience may result in a longer convergent time. Finally, due to the fuzzy formulations of the output signals, proposed schemes hold the capability of imposing saturation bounds on the output control effort.

Acknowledgements

The authors are greatly indebted to the National Science Council of ROC for the support of the research through contact Nos. NSC 89-2213-E-033-044 and NSC 89-2218-E-033-024.

References

[1] G.F. Garrier, On the nonlinear vibration problem of the elastic string, Quarterly of Applied Mathematics 3 (1945) 157–165.
[2] C.D. Mote Jr., Dynamic stability of axially moving materials, Shock Vibration Digest 4 (1972) 2–11.
[3] J.A. Wicker, C.D. Mote Jr., On the energetics of axially moving continua, Journal of Acoustical Society of America 85 (1989) 1365–1368.
[4] J.A. Wicker, C.D. Mote Jr., Classical vibration analysis of axially moving continua, American Society of Mechanical Engineers, Journal of Applied Mechanics 57 (1990) 738–744.
[5] S.Y. Lee, C.D. Mote Jr., A generalized treatment of the energetics of translating continua, Part I: strings and second order tensioned pipes, Journal of Sound and Vibration 204 (5) (1997) 717–734.
[6] J.S. Chen, Natural frequencies and stability of an axially translating string in contact with a stationary load system, American Society of Mechanical Engineers, Journal of Vibration and Acoustics 119 (1997) 152–157.
[7] G. Chen, Energy decay estimates and exact boundary value controlliability for the wave equation in a bounded domain, Journal de Mathématiques Pures Appliquées 58 (1979) 249–273.
[8] A.E. Jai, A.J. Pritchard, Sensors and actuators in distributed systems, International Journal of Control 46 (1987) 1139–1153.
[9] B. Yang, C.D. Mote Jr., Active vibration control of the axially moving string in the s domain, American Society of Mechanical Engineers, Journal of Applied Mechanics 58 (1991) 189–196.
[10] C.H. Chung, C.A. Tan, Active vibration control of the axially moving string by wave cancellation, American Society of Mechanical Engineers, Journal of Vibration and Acoustics 117 (1995) 49–55.
[11] S.Y. Lee, C.D. Mote Jr., Vibration control of an axially moving string by boundary control, American Society of Mechanical Engineers, Journal of Dynamics Systems, Measurement, and Control 118 (1996) 66–74.
[12] R.F. Fung, C.C. Tseng, Boundary control of an axially moving string via Lyapunov method, American Society of Mechanical Engineers, Journal of Dynamics Systems, Measurement, and Control 121 (1999) 105–110.
[13] R. Palm, Robust control by fuzzy sliding mode, Automatica 30 (1994) 1429–1437.
[14] R.R. Yager, D.P. Filev, Essentials of Fuzzy Modeling and Control, Wiley, New York, 1994.

[15] Y.S. Lu, J.S. Chen, A self-organizing fuzzy sliding mode controller design for a class of nonlinear servo system, IEEE Transactions on Industrial Electronics 41 (1994) 492–502.
[16] J.C. Wu, T.S. Liu, A sliding mode approach to fuzzy control design, IEEE Transactions on Control Systems Technology 4 (1996) 141–151.
[17] R.F. Fung, C.C. Saw, A.P. Wang, Region-wise linear fuzzy sliding mode control of the motor-mechanism systems, Journal of Sound and Vibration 234 (3) (2000) 471–489.
[18] C.C. Lee Fuzzy, Logic in control systems: fuzzy logic controller—Part I and Part II, IEEE Transactions on Systems, Man, and Cybernetics 20 (2) (1990) 404–436.
[19] L.X. Wang, Adaptive Fuzzy Systems and Control: Design and Stability Analysis, Prentice-Hall, Englewood Cliffs, NJ, 1994.
[20] S. Commuri, F.L. Lewis, Adaptive fuzzy logic control of robot manipulators, IEEE Transactions on Robotics and Automation 3 (1996) 2604–2609.
[21] T. Fukuda, T. Shibata, Theory and applications of neural networks for industrial control systems, IEEE Transactions on Industrial Electronics 39 (6) (1992) 472–489.
[22] P.S. Sastry, G. Santharam, K.P. Unnikrishnan, Memory neuron networks for identification and control of dynamical systems, IEEE Transactions on Neural Networks 5 (2) (1994) 306–319.
[23] Y. Zhang, P. Sen, G.E. Henran, An on-line trained adaptive neural controller, IEEE Control Systems Magazine 15 (5) (1995) 67–75.
[24] C.C. Ku, K.Y. Lee, Diagonal recurrent networks for dynamic systems control, IEEE Transactions on Neural Networks 6 (1) (1995) 144–156.
[25] C.T. Lin, C.S.G. Lee, Neural-network-based fuzzy logic control and decision system, IEEE Transactions on Communications 40 (12) (1991) 1320–1336.
[26] S. Horikawa, T. Furuhashi, Y. Uchikawa, On fuzzy modelling using fuzzy neural networks with the backpropagation algorithm, IEEE Transactions on Neural Networks 3 (5) (1992) 801–806.
[27] A. Ismael, B. Hussien, R.W. Mclaren, Fuzzy neural network implementation of self tuning PID control, IEEE International Symposium on Intelligent Control, 1994, pp. 16–21.
[28] Y.C. Chen, C.C. Teng, A model reference control structure using a fuzzy neural network, Fuzzy Sets and Systems 73 (1995) 291–312.
[29] J. Zhang, A.J. Morris, Fuzzy neural networks for nonlinear systems modelling, IEE Proceedings of the Control Theory and Applications 6 (1995) 551–556.
[30] T.S.R. Jang, C.T. Sun, Neural-fuzzy modeling and control, Proceedings of the IEEE 83 (3) (1995) 378–405.
[31] S.C. Lin, Y.Y. Chen, Design of self-learning fuzzy sliding mode controllers based in genetic algorithms, Fuzzy Sets and Systems 86 (1997) 139–153.
[32] F.J. Lin, W.J. Hwang, R.J. Wai, A supervisory fuzzy neural network control system for tracking periodic inputs, IEEE Transactions on Fuzzy Systems 7 (1) (1999) 41–52.
[33] N.S. Abhyankar, E.K. Hall, S.V. Hanagud, Chaotic vibration of beams: numerical solution of partial differential equations, American Society of Mechanical Engineers, Journal of Applied Mechanics 60 (1) (1993) 167–174.